DALTON
FULL PAPER

Compositions and conformations of several transition metal complexes with a nonapeptide hormone oxytocin †

Hua Wei, Xuemei Luo, Yibing Wu, Yong Yao, Zijian Guo and Longgen Zhu *

State Key Laboratory of Coordination Chemistry, Coordination Chemistry Institute, Nanjing University, Nanjing, 210093, P. R. China

Received 30th May 2000, Accepted 12th September 2000
First published as an Advance Article on the web 27th October 2000

Similar co-ordination characteristics of oxytocin (OT) towards Cu^{II}, Ni^{II}, Mn^{II} and Zn^{II} at different pH values have been demonstrated by electrospray mass spectrometry (ESMS) and rationalized by molecular mechanics simulation. At *ca.* pH 2 oxytocin does not interact with the metal ions; at pH 5 species with metal bound oxytocin were detected, including $[OT + H^+]^+$, $[M + OT]^{2+}$, $[M + OT - H^+]^+$, $[M + OT + ClO_4^- + H^+]^{2+}$ and $[M + OT + ClO_4^-]^+$ and only stable 4N complexes were found at pH ≈ 9. Molecular modelling studies using the Universal force field (UFF) showed that the four N-donor centers of oxytocin prefer the square planar geometry in complexes of Ni^{II} and Mn^{II}. For Pd^{II}, the Sγ(1) co-ordinated conformer was found to be more stable than the Sγ(6) co-ordinated one. Dramatic conformational changes occur upon oxytocin co-ordinating to Ni^{II}, Mn^{II} or Pd^{II}.

Many naturally occurring peptides do not have a purely organic mode of action; some are activated or biotransformed by metal ions, others show metal-dependent regulation or metabolism.[1–3] Oxytocin is a physiologically important nonapeptide, containing a 20-membered tocin ring (from Cys-1 to Cys-6) and an acyclic tripeptide tail (from Pro-7 to Gly-9).[4,5] The cyclic structure is completed by the formation of a disulfide bond between Cys-1 and Cys-6 (Scheme 1). Structural investigations[6–10] revealed that the conformation of oxytocin consists of two β turns: one in the cyclic moiety involving the sequence Tyr2-Ile3-Gln4-Asn5, and another, a hairpin turn, involving the C-terminal sequence Cys6-Pro7-Leu8-Gly9.

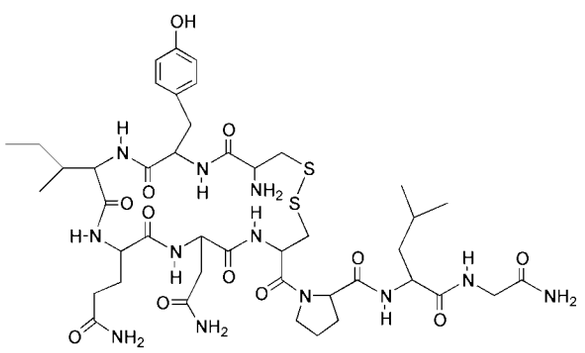

Scheme 1 Molecular structure of oxytocin.

Many metal ions including essential elements have been found to form complexes with oxytocin and its analogues.[11–19] It was reported that Cu^{II} and Ni^{II} form unusually stable square planar complexes with four N co-ordination (4N complexes) at pH above 8 and 9, respectively,[13–15] and that Mn^{II} co-ordinates to amide carbonyls of Asn-5, Gly-9 in addition with the peptide carbonyl of Thr-4 or the amide carbonyl of Gln-4.[16] It is well known that the co-ordination of metal ions to peptides affects the conformation dramatically and that the characteristic conformation of a peptide is essential for ligand–receptor interaction. Therefore, it is to be expected that the agonist activity of oxytocin and its analogues will be affected by metal ion co-ordination. However, detailed conformational information on metal complexes with oxytocin and its analogues is rare.

ESMS has been shown to be a useful technique for analysing multiply charged ions, such as large biomolecules[20] and metal complexes.[21,22] Recently, the technique has been used to study the interaction of metal ions with peptides.[11,12] It proved to be a powerful tool for this kind of study too. The intact ions formed by interaction of metal ions with peptides are always observed, emphasizing the "soft" nature of the ESMS process.

Based on classic work, popular force fields are limited to particular combinations of atoms, for example those of proteins, organics, or nucleic acids. An entirely new force field, UFF,[23] was used here. The set of fundamental parameters in UFF is based only on the element, its hybridization and connectivity, thus this force field can be extended to the entire Periodic Table. The lowest energy conformations and energy differences between conformers calculated using UFF are quite close to the experimental ones.

In the present article, we report ESMS studies of the interaction of metal ions with oxytocin. A variety of structural information has been obtained by precise determination of molecular masses and isotope distribution patterns. To ascertain how metal ions affect the peptide conformation, molecular mechanics calculations were performed for oxytocin 4N complexes with Ni^{II} and Mn^{II} as well as the palladium(II) oxytocin complex $[Pd(en)(OT)]^{2+}$ (en = ethylenediamine).

Materials and methods

Experimental

Doubly distilled water was used for preparation of solutions. Oxytocin was purchased from Fluka. All other chemicals were of reagent grade. The molecular mass of oxytocin was measured to be 1007.5 with isotopic peaks separated by 1.0 *m*/*z* unit; calculated value for $[OT + H^+]^+$ 1007.4.

Solutions containing 2 mmol l^{-1} metal ion (perchlorate salt of Cu^{II}, Ni^{II}, Mn^{II} or Zn^{II}) and 1 mmol l^{-1} oxytocin were adjusted to different pH values by $HClO_4$ or NaOH solutions, followed by ESMS determination of the solution species. An LCQ electrospray mass spectrometer (ESMS, Finnigan) was employed. The sample was loaded into the injection valve, injected into a mobile phase solution of 50% aqueous methanol containing 1% acetic acid and carried through the electrospray

† Electronic supplementary information (ESI) available: conformation of complex **4**, hydrogen bond parameters for oxytocin and its palladium(II) complex. See http://www.rsc.org/suppdata/dt/b0/b004254o/

 DOI: 10.1039/b004254o

interface into the mass analyzer at a rate of 200 μl min^{-1}. The voltage at the electrospray needles was 5 kV and the capillary was heated to 200 °C. A maximum ion injection time of 0.2 s along with 10 scans was set. Zoom scan was used in these experiments. The isotope distribution pattern for each complex was calculated by the IsoPro 3.0 program.[24] The pH value was measured by an Orion 901 pH meter with a phoenix Ag–AgCl reference electrode.

Molecular mechanics modelling

The nuclear Overhauser enhancement (NOE) distance constraints of oxytocin were taken from ref. 6 (half are lower limits, half are upper limits), 85 of which were found to be meaningful for the structure calculation. The solution structures were calculated by the DYANA program.[25] 100 initial structures were randomly selected, followed by 15000 steps of cooling calculation, and 10 structures with the lowest NOE target function were obtained. Restricted energy minimization (REM) was then performed upon these 10 structures using the SANDER program,[26] and the structure with the lowest average energy was the final solution structure of oxytocin (**1**).

Metal ions were then docked to compound **1** with the removal of peptide protons if necessary so that complexes with the following formulae were obtained: $[Ni(N,N,N,N\text{-}OTH_{-3})]^-$ **3**, $[Mn(N,N,N,N\text{-}OTH_{-3})]^-$ **4**, $[Mn(N,N,N,N,O,O\text{-}OTH_{-3})]^-$ **5**, $[Pd(en)(N,S^1\text{-}OT)]^{2+}$ **6**, $[Pd(en)(N,S^6\text{-}OT)]^{2+}$ **7**. In **3** and **4**, Ni^{II} and Mn^{II} co-ordinate to the amino N of Cys-1 and the peptide N atoms of Tyr-2, Ile-3 and Gln-4. In **5**, two extra carbonyl O atoms attach to Mn^{II} through axial co-ordination so that Mn^{II} is octahedrally co-ordinated. In **6**, Pd^{II} co-ordinates to the amino N of Cys-1, S atom of the Cys-1 side chain and two amino N atoms of en. In **7** the S atom of the Cys-6 side chain replaces that of Cys-1, the other three co-ordination atoms being the same as those of **6**. Pd^{II} in **6** and **7** has a square planar environment. The geometries of **3**, **4** (both tetrahedral and square planar), **5**, **6** and **7** were optimized by the Universal 1.02 force field.[23] Although a shell of water molecules may have some effect on the structure of oxytocin metal complexes, water molecules were not explicitly added due to the difficulty of accurately simulating the water shell. Since UFF contains only copper(I) parameters, the copper(II) complex of oxytocin was not geometry-optimized in this report. To be comparable to oxytocin metal complexes, **1** was also geometry-optimized by UFF and the obtained structure referred to as **2**.

Empirical energy functions were used which include harmonic potential-energy terms for bond lengths, bond angles, torsion angles, inversions and functions for van der Waals and electrostatic interactions. The usual convention was followed, which excludes van der Waals and electrostatic interactions for atoms that are bonded to each other (1,2 interactions) or to a common atom (1,3 interactions). A spline scheme was used for long-range interactions, and the real space spline-on and spline-off distances are 11.0 and 14.0 Å, respectively. A non-bond list with 2.0 Å buffer was also used. The Smart Minimizer algorithm was used to search for the minimum of the energy space, and the convergence criterion was set to 1.0×10^{-4} kcal mol^{-1}. After each cycle of energy minimization, partial charges of all the atoms were recalculated using the Qeq-charged 1.1 charge equilibration scheme[27] and the convergence criterion was set to 5.0×10^{-4} e. Final structures with the lowest energy were obtained when self-consistency between the partial charges and energy was achieved. The molecular graphics software Cerius2[28] was used for the generation, display, analysis and plotting of the molecular structures.

Results and discussion

From the ESMS results it was found that the co-ordination characteristics of Cu^{II}, Ni^{II}, Mn^{II} and Zn^{II} are very similar. The detected species at different pH values are listed in Table 1, together with the *m*/*z* value of the lightest isotopic species. At *ca.* pH 2 no interaction was found between the metal ions and oxytocin; $[OT + H^+]^+$ was the only species detected. At *ca.* pH 5 many species were detected, including $[OT + H^+]^+$, $[M + OT]^{2+}$, $[M + OT - H^+]^+$, $[M + OT + ClO_4^- + H^+]^{2+}$ and $[M + OT + ClO_4^-]^+$. No negatively charged species was detected. The ESMS spectrum of the Cu^{II}–oxytocin system at pH 4.93 is shown in Fig. 1. From the separation of the isotopic peaks and their *m*/*z* values, the charges and molecular masses of the species can be deduced. All the five species shown above were detected. Besides free oxytocin, the most abundant species is $[Cu+OT]^{2+}$. It is likely that Cu^{II} co-ordinates to the amino N of Cys-1 and carbonyl oxygen atoms of several residues in $[Cu + OT]^{2+}$.

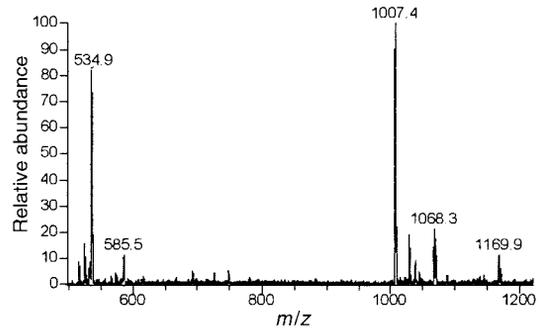

Fig. 1 ESMS spectrum of oxytocin–Cu^{II} system at pH 4.93.

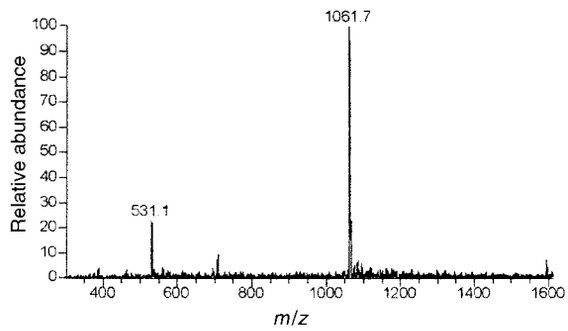

Fig. 2 ESMS spectrum of oxytocin–Ni^{II} system at pH 8.92.

At *ca.* pH 9, Cu^{II}, Ni^{II} and Mn^{II} form stable complexes with oxytocin; only the 4N complexes were detected. The ESMS spectrum of the Ni^{II}–oxytocin system at pH 8.92 is shown in Fig. 2. Two species, **3** and $[Ni(N,N,N,N\text{-}OTH_{-4})]^{2-}$, were detected. The latter species differs from the former only by deprotonation of the phenolic group of the Tyr-2 residue. Fig. 3 (A) gives the detected isotopic peaks of **3**. From their separations, which were 1.0 *m*/*z* unit, the corresponding species is a singly charged anionic complex. Fig. 3(B) shows the simulated spectrum which fits Fig. 3(A) very well. Since amino N is more nucleophilic than amide N, one of the co-ordination atoms in 4N complexes must be the amino N of Cys-1. Metal ion co-ordination to the amino N of Cys-1 will then facilitate binding of the peptide N of Tyr-2 to the metal ion due to its vicinity. With increase of pH, the peptide N atoms of Ile-3 and Gln-4 will co-ordinate cooperatively because of their advantageous positions.[13–15] Therefore, it is likely that in the 4N complexes the metal ion co-ordinates to the amino N of Cys-1 and the peptide N atoms of Tyr-2, Ile-3 and Gln-4.

For the final REM family of 10 structures, the root mean square differences for backbone atoms and for all heavy atoms were 0.69 ± 0.37 and 1.06 ± 0.41 Å, respectively. The NOE average target function was 0.37 ± 0.03 $Å^2$. There were no residues in disallowed Ramachandran plot regions, and 83.3% of the residues were in most favored or allowed Ramachandran plot regions. From ESI supplementary material, there is a hydrogen bond between the peptide H–N of Gly-9 and the CO of Cys-6 in compound **1**, which promotes the formation of the

Table 1 ESMS observed species during the reaction of oxytocin with Cu^{II}, Ni^{II}, Mn^{II} and Zn^{II} at different pH

Ion	pH	Species detected and their *m*/*z*
Cu^{II}	2.04	$[OT + H^+]^+$ (1007.4)
	4.93	$[OT + H^+]^+$ (1007.4), $[Cu + OT]^{2+}$ (534.9), $[Cu + OT - H^+]^+$ (1068.3), $[Cu + OT + ClO_4^-]^+$ (1167.9), $[Cu + OT + ClO_4^- + H^+]^{2+}$ (584.5)
	8.98	$[Cu(N,N,N,N - OTH_{-3})]^-$ (1066.8)
Ni^{II}	2.07	$[OT + H^+]^+$ (1007.5)
	5.10	$[OT + H^+]^+$ (1007.5), $[Ni + OT]^{2+}$ (532.3), $[Ni + OT - H^+]^+$ (1063.3), $[Ni + OT + ClO_4^-]^+$ (1163.1), $[Ni + OT + ClO_4^- + H^+]^{2+}$ (582.5)
	8.92	$[Ni(N,N,N,N - OTH_{-3})]^-$ (1061.3)
Mn^{II}	2.02	$[OT + H^+]^+$ (1007.3)
	5.09	$[OT + H^+]^+$ (1007.3), $[Mn + OT]^{2+}$ (530.9), $[Mn + OT - H^+]^+$ (1060.3), $[Mn + OT + ClO_4^-]^+$ (1159.9), $[Mn + OT + ClO_4^- + H^+]^{2+}$ (580.4)
	8.92	$[Mn(N,N,N,N - OTH_{-3})]^-$ (1058.8)
Zn^{II}	1.89	$[OT + H^+]^+$ (1007.3)
	5.04	$[OT + H^+]^+$ (1007.3), $[Zn + OT]^{2+}$ (535.3), $[Zn + OT - H^+]^+$ (1069.4), $[Zn + OT + ClO_4^-]^+$ (1169.1), $[Zn + OT + ClO_4^- + H^+]^{2+}$ (585.0)
	9.05	—

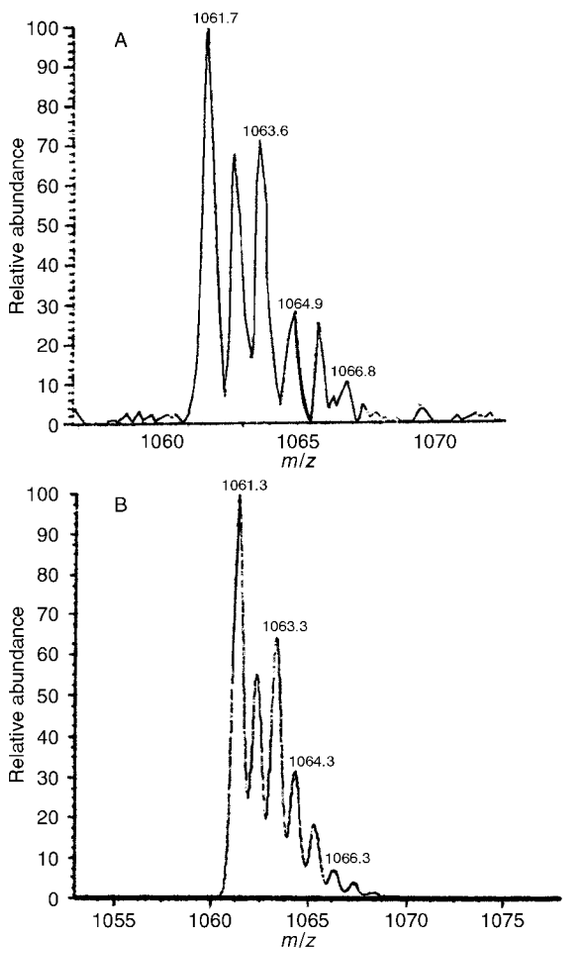

Fig. 3 (A) Isotopic peaks of the 4N complex of Ni^{II} with oxytocin (**3**). (B) Simulated isotopic peaks of $C_{43}H_{63}N_{12}NiO_{12}S_2$.

β-turn conformation covering the residues Cys6-Pro7-Leu8-Gly9. However, no hydrogen bond was found between Tyr-2 and Asn-5, which may be caused by the shortcomings of the Amber force field. All hydrogen bonds were found to be relatively weak due to the imperfection of UFF.

The conformation of compound **2** is shown in Fig. 4. From Table 2 it can be seen that many changes in the main chain, side chain and disulfide torsion angles were observed compared to **1**. The disulfide torsion angle changed from −138.1° with left-handed chirality to 137.1° with right-handed chirality. A hydrogen bond directed from Asn-5 to Tyr-2 was found in the new structure and the hydrogen bond from Gly-9 to Cys-6 in the original structure was replaced by one from Leu-8 to Cys-6.

In order to know whether the four N-donor centers are

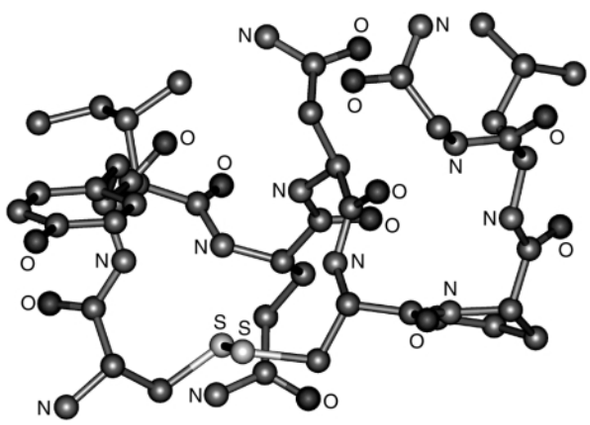

Fig. 4 Conformation of oxytocin (**2**) optimized by UFF.

square planarly or tetrahedrally located, both types of complexes of Ni^{II} and Mn^{II} were energy-minimized. In the calculation of the tetrahedral complexes five angles around each metal ion were restrained to 109.5° (the force constants were 1000 kcal mol^{-1} rad^{-1}). It was found that the square planar complexes were much more stable than the corresponding tetrahedral complexes. For Ni^{II} the total energy of the tetrahedral complex was 132.5 kcal mol^{-1}, and the restraint energy was 65.3 kcal mol^{-1}, while the total energy of the square planar complex was −25.5 kcal mol^{-1}. For Mn^{II} the total energy of the tetrahedral complex was 111.0 kcal mol^{-1}, the restraint energy 57.3 kcal mol^{-1}, while the total energy of the square planar complex was −34.5 kcal mol^{-1}. In both complexes the four N-donor atoms deviate significantly from an ideal tetrahedral structure. Three are almost at three corners of a square, whose center is occupied by the metal ion. The line passing through the fourth N atom and the metal ion is nearly perpendicular to the square plane. The large distortion can also be seen from the large restraint energies. Therefore it is reasonable to assume that the four N-donor centers are square planarly located in both 4N complexes of Ni^{II} and Mn^{II}. The energy minimized structures of **3** and **4** are shown in Fig. 5 and as supplementary material. The average Ni–N bond length of **3** is 1.83 Å, very close to the value of 1.87 Å of an oxamide oxime complex of Ni^{II}.[29] The largest deviation from 90.0° for the four angles around Ni^{II} is 5.0°. The average Mn–N bond length of **4** is 1.95 Å, 0.30 Å lower than the crystal value of an imidazole complex of Mn^{II}.[30] The relatively large difference is probably caused by the lack of parameters for the Mn–N bond length in UFF. The largest deviation from 90.0° for the four angles around Mn^{II} is 7.9°.

It can be seen from Table 2 that dramatic changes of the conformation of oxytocin (**2**) occur after it co-ordinates to Ni^{II} or Mn^{II} in the 4N complexes, which suggests that the potential N-donor centers in oxytocin are not ideally situated for square

Table 2 Torsion angles (°) for the backbone and side chain (about the Cα–Cβ bond) in oxytocin and its complexes

Residue	Angle*	**1**	**2**	**3**	**4**	**5**	**6**
Cys-1	ψ	126.9	158.1	−20.7	−16.2	−26.3	121.1
	χ	117.3	−178.3	−80.2	−76.4	−60.3	−54.1
	φ	−145.8	−99.1	176.1	175.8	−163.2	−79.0
Tyr-2	ψ	80.4	69.9	5.5	2.5	2.8	116.6
	χ	−35.5	−52.4	−144.4	−100.7	−138.0	−58.5
	φ	89.4	74.3	−170.0	−177.2	−163.1	39.1
Ile-3	ψ	43.3	14.9	−9.1	−9.6	11.9	47.3
	χ	−137.5	−132.6	−172.3	−174.0	−166.6	−167.2
	φ	−65.1	76.7	83.1	67.4	80.3	59.1
Gln-4	ψ	19.1	29.8	−70.9	−65.4	−53.8	48.6
	χ	−94.0	−52.1	−48.1	−138.4	−28.6	−134.7
	φ	−63.4	−87.8	−60.2	−61.9	−45.3	−107.3
Asn-5	ψ	12.9	7.7	111.3	115.2	82.3	64.8
	χ	−113.2	−74.3	−84.5	−69.8	−77.8	−71.2
	φ	−45.7	−61.8	−115.2	−120.0	−51.8	−121.0
Cys-6	ψ	−58.8	−36.9	−60.8	−64.7	−58.8	−70.3
	χ	−110.9	−70.3	−177.0	−176.3	134.2	−78.4
	φ	−75.0	−84.4	−72.5	−73.2	−109.9	−78.3
Pro-7	ψ	96.3	66.1	−8.1	−5.0	−5.5	−17.2
	χ	18.6	30.1	23.3	25.2	34.5	27.8
	φ	159.7	−168.9	−94.5	−96.0	−149.6	−72.0
Leu-8	ψ	−25.9	−56.9	−57.0	−54.6	−56.2	−50.1
	χ	151.5	−156.3	177.5	173.8	180.0	173.4
Gly-9	φ	180.0	111.3	−130.4	−130.4	−69.1	179.5
Disulfide torsion		−138.1	137.1	−102.0	−98.1	−103.8	−115.0

* Angles φ, ψ, χ are defined according to IUPAC nomenclature, *i.e.* $\varphi^i = \tau(C_C^{i-1}–N^i–C_\alpha^i–C_C^i)$, $\psi^i = \tau(N^i–C_\alpha^i–C_C^i–N^{i+1})$, $\chi^i = \tau(N^i–C_\alpha^i–C_\beta^i–C_\gamma^i)$; C_C^i is carboxylic C of the *i*th residue.

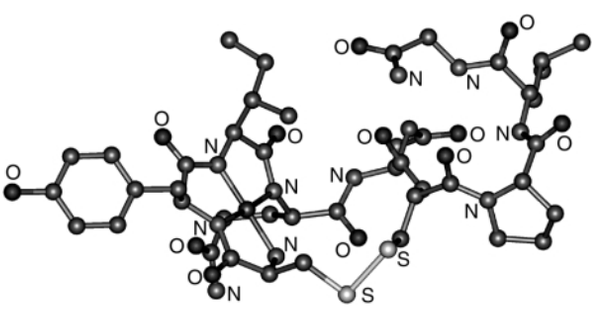

Fig. 5 Conformation of the 4N complex of Ni^{II} with oxytocin (**3**).

planar co-ordination, contrary to previous conjecture.[13–15] Although the three amide N atoms are nearly at the three corners of a square, the amino N of Cys-1 projects outside and is far away from the fourth corner. Owing to the critical position of Tyr-2,[31–33] special attention was given to its side chain orientation relative to the tocin ring. In oxytocin the aromatic ring of Tyr-2 is almost folded back over the tocin ring. Upon co-ordination to Ni^{II} or Mn^{II} it moves away from the top of the tocin ring, but still remains roughly parallel to it, while the peptide carbonyl of Tyr-2 projects away from the metal ion, which precludes its participation in hydrogen bonding. The hydrogen bond directed from Cys-6 to Leu-8 also disappears.

The conformations of complexes **3** and **4** are very similar due to their similarity in co-ordination mode. However, differences still exist. In **3** the aromatic ring of Tyr-2 moves further away from the top of the tocin ring than in **4**. The difference of the Gln-4 side chain torsion angle between **3** and **4** is very large, 90.3°. Differences of other torsion angles between **3** and **4** are relatively small. In both **3** and **4** no hydrogen bond was observed.

Usually Mn^{II} has an octahedral geometry. ESMS is able to reveal co-ordinated water molecules,[11,34] but none was detected for the oxytocin complex with Mn^{II} and it is unlikely that water molecules occupy the axial positions. On the other hand, it is possible that the carbonyl O atoms of oxytocin participate in the co-ordination, as reported before.[16] From the figure in ESI it can be seen that the amide O of Gln-4 is the only one able to occupy the "outer" axial position. However, many carbonyl O atoms can occupy the "inner" axial position, including peptide

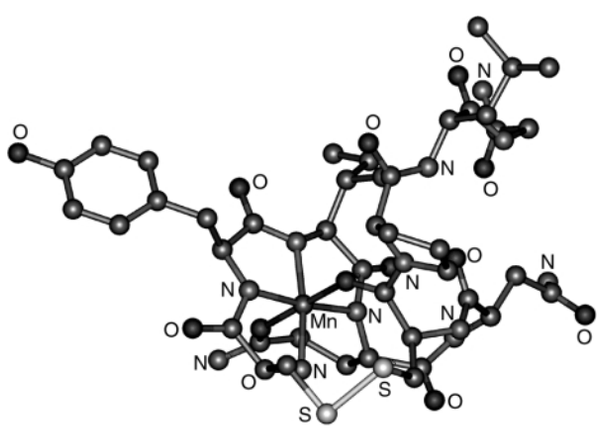

Fig. 6 Conformation of the octahedrally co-ordinated manganese(II) complex with oxytocin (**5**).

O of Gln-4, amide and peptide O of Asn-5, peptide O of Cys-6, Pro-7, Leu-8 and Gly-9. All these possible configurations were geometry-optimized. Their energies are −2.5, −111.0, −109.7, −135.8, −109.6, −74.9 and −124.4 kcal mol^{-1}, respectively. The energy of the configuration which has the peptide O of Cys-6 at the "inner" axial position is considerably lower than that of any other one, and it is also much lower than that of the square planar configuration. Therefore, at *ca.* pH 9, oxytocin co-ordinates to Mn^{II} octahedrally, with four N atoms at four corners of a square and the amide O of Gln-4 together with the peptide O of Cys-6 at the axial positions (**5**). The optimized conformation of **5** is shown in Fig. 6. It can clearly be seen that dramatic conformational changes occur when the manganese(II) complex with oxytocin changes from square planar to octahedral. The position of the aromatic ring of Tyr-2 in **5** is similar to that of **3**. No hydrogen bond was found in **5**. The oxytocin complex with Mn^{II} that has two water molecules at the axial positions was also geometry-optimized, in case that the co-ordinated water molecules were lost before ESMS detection. The relative orientation of the aromatic ring of Tyr-2 in this complex is similar to that of **5**, however the backbone atoms are much more extended since carbonyl O atoms no longer co-ordinate to Mn^{II}.

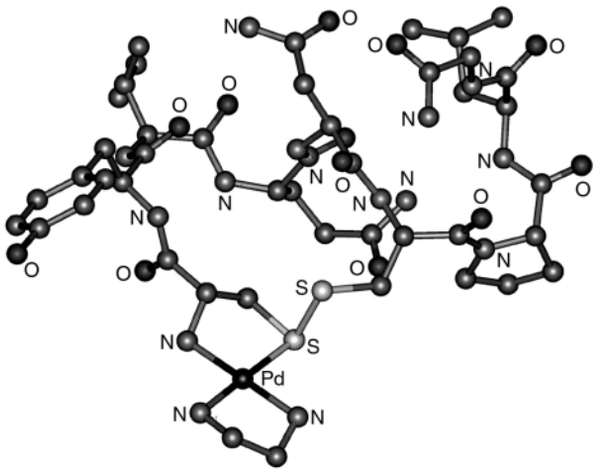

Fig. 7 Conformation of $[Pd(en)(N,S^1\text{-OT})]^{2+}$ **6**.

We have previously reported that Pd^{II} co-ordinated to oxytocin *via* one of the two S atoms of the disulfide bridge,[11] but were unable to decide between the two. To answer this question both complexes **6** and **7** were geometry-optimized. The total energy of **6** was −32.40 kcal mol^{-1}, which is 3.09 kcal mol^{-1} lower than that of **7**. The largest deviation from 90.0° for the four angles around Pd^{II} in **7** is 4.6°, which is 2.4° larger than that of **6**. Therefore, we can conclude that **6** is likely the more preferred structure, although the energy and angle deviation differences between **6** and **7** are rather small. The optimized structure of **6** is shown in Fig. 7.

The Pd–S bond length and the average Pd–N bond length are 2.35 and 1.99 Å, respectively, which are only 0.09 and 0.04 Å smaller than the crystal values of $[Pd(Met)Cl_2]$.[35] Co-ordination of Pd^{II} to oxytocin also causes dramatic changes to its conformation. The side chain torsion angle of Cys-1 gives the relative position of the amino N atom and side chain S atom to the Cα(1)–Cβ(1) bond. The two atoms need to be on the same side of the bond to make a concerted co-ordination. However, in free oxytocin they are in *trans* position around the bond, so the conformation of oxytocin must change a lot to be suitable for co-ordination with Pd^{II}. The conformation of **6** is also much different from that of oxytocin complexes with Ni^{II} and Mn^{II}. In **6** the aromatic ring of Tyr-2 moves only slightly away from the top of the tocin ring. Since the peptide N atoms do not participate in the co-ordination in **6**, the hydrogen bond between the CO of Tyr-2 and the peptide H–N of Asn-5 is preserved. Two new hydrogen bonds are formed: one between the CO of Tyr-2 and the amide H–N of Asn-5, the other between the CO of Cys-6 and the amide H–N of Gly-9.

Conclusion

Although at *ca.* pH 5 many metal-bound oxytocin species were detected, 4N complexes, which were confirmed for Cu^{II} and Ni^{II} by other methods, were the only species observed at *ca.* pH 9. Molecular mechanics simulation revealed that that of Ni^{II} is square planar, while that of Mn^{II} is octahedral and the Sγ(1) co-ordinated conformer of Pd^{II} is more stable than the Sγ(6) co-ordinated one.

It is proved that co-ordination of metal ions to oxytocin dramatically changes its conformation. The disulfide torsion angle changed from right-handed chirality in **2** to left-handed chirality in complexes **3**, **4**, **5** and **6**. There was little change in the position of the aromatic ring of Tyr-2 for **6**, but it moved considerably away from the top of the tocin ring in **3**, **4** and **5**. The metal ion co-ordination to oxytocin decreases its flexibility and the interconvertibility between left- and right-handed conformers, which will lead to a decrease in its agonist activity, and the large change in the position of the aromatic ring of Tyr-2 may have the same effect. On the other hand, the left-handed conformer was stabilized in all four metal complexes with oxytocin, which will lead to an increase in its agonist activity.[7] These conformational details of the oxytocin complexes are likely to contribute to further understanding of the recognition of oxytocin by its receptors.

Acknowledgements

This work was supported by the National Natural Science Foundation of China (Nos. 29871017 and 29823001).

References

1 E. Lodyga-Chruscinska, G. Micera, D. Sanna, J. Olczak, J. Zabrocki, H. Kozlowski and L. Chruscinski, *J. Inorg. Biochem.*, 1999, **76**, 1.
2 P. Gouet, B. Fabry, V. Guillet, C. Birck, L. Mourey, D. Kahn and J.-P. Samama, *Structure* (*London*), 1999, **7**, 1517.
3 M. Kalafatis, J. O. Egan, C. Van't Veer, K. M. Cawthern and K. G. Mann, *Crit. Rev. Eukaryotic Gene Expression*, 1997, **7**, 241.
4 P. F. Levay, M. Viljoen and H. S. Meij, *S. Afr. Tydskr. Natuurwet. Tegnol.*, 1993, **12**, 61.
5 K. Uvnaes-Moberg, *Ann. Med.* (*Helsinki*), 1994, **26**, 315.
6 R. Bhaskaran, L. Chuang and C. Yu, *Biopolymers*, 1992, **32**, 1599.
7 S. P. Wood, I. J. Tickle, A. M. Treharne, J. E. Pitts, Y. Mascarenhas, J. Y. Li, J. Husain, S. Cooper, T. L. Blundell, V. J. Hruby, A. Buku, A. J. Fischman and H. R. Wyssbrod, *Science*, 1986, **232**, 633.
8 V. J. Hruby, *Trends Pharm. Sci.*, 1987, **8**, 336.
9 M. Lebl, P. Hill, W. Kazmierski, L. Karaszova, J. Slaninova, I. Fric and V. J. Hruby, *Int. J. Pept. Protein Res.*, 1990, **36**, 321.
10 D. Cowburn, D. H. Live, A. J. Fischman and W. D. Agosta, *J. Am. Chem. Soc.*, 1983, **103**, 7435.
11 X. Luo, W. Huang, Y. Mei, S. Zhou and L. Zhu, *Inorg. Chem.*, 1999, **38**, 1474.
12 A. D'Agostino, R. Colton, J. C. Traeger and A. J. Canty, *Eur. Mass Spectrom.*, 1996, **2**, 273.
13 P. Danyi, K. Várnagy, I. Sóvágó, I. Schön, D. Sanna and G. Micera, *J. Inorg. Biochem.*, 1995, **60**, 69.
14 W. Bal, H. Kozlowski, B. Lammek, L. D. Pettit and K. Rolka, *J. Inorg. Biochem.*, 1992, **45**, 193.
15 H. Kozlowski, B. Radomska, G. Kupryszewski, B. Lammek, C. Livera, L. D. Pettit and S. Pyburn, *J. Chem. Soc.*, *Dalton Trans.*, 1989, 173.
16 G. Valensin, A. Maccotta, E. Gaggelli, A. Grzonka, G. Kasprzykowski and H. Kozlowski, *Eur. J. Biochem.*, 1996, **240**, 118.
17 V. S. Ananthanarayanan and K. S. Brimble, *Biopolymers*, 1996, **40**, 433.
18 V. S. Ananthanarayanan, M.-P. Belciug and B. S. Zhorov, *Biopolymers*, 1996, **40**, 445.
19 M. Rholam, P. Nicolas and P. Cohen, *Biochemistry*, 1985, **24**, 3345.
20 C. M. Fenwick and A. M. English, *J. Am. Chem. Soc.*, 1996, **118**, 12236.
21 A. Marrquis-Rigault, A. Dupont-Gervais, P. N. Baxler, A. van Dorsselaer and J.-M. Lehn, *Inorg. Chem.*, 1996, **35**, 2307.
22 C. Moucheron and A. K.-D. Mesmaeker, *J. Am. Chem. Soc.*, 1996, **118**, 12834.
23 A. K. Rappé, C. J. Casewit, K. S. Colwell, W. A. Goddard-III and W. M. Skiff, *J. Am. Chem. Soc.*, 1992, **114**, 10024.
24 J. A. Yergey, *Int. J. Mass Spectrom. Ion Phys.*, 1983, **52**, 337.
25 P. Güntert, C. Mumenthaler and K. Wüthrich, *J. Mol. Biol.*, 1997, **273**, 283.
26 D. A. Pearlman and D. A. Case, SANDER, University of California, San Francisco, CA, 1991.
27 A. K. Rappé and W. A. Goddard-III, *J. Phys. Chem.*, 1991, **95**, 3358.
28 Cerius 2, Molecular Simulation Inc., 1997.
29 H. Endres and M. Schendzielorz, *Acta Crystallogr.*, *Sect. C*, 1983, **39**, 1528.
30 T. P. J. Garrett, J. M. Guss and H. C. Freeman, *Acta Crystallogr.*, *Sect. C*, 1983, **39**, 1031.
31 J. P. Rose, C.-K. Wu, C.-D. Hsiao, E. Breslow and B.-C. Wang, *Nat. Struct. Biol.*, 1996, **3**, 163.
32 S. Oldziej, J. Ciarkowski, A. Liwo, M. D. Shenderovich and Z. J. Grzonka, *Recept. Signal Transduction Res.*, 1995, **15**, 703.
33 S. Liao, M. D. Shenderovich, Z. Zhang, L. Maletinska, J. Slaninova and V. J. Hruby, *J. Am. Chem. Soc.*, 1998, **120**, 7393.
34 X. Luo, W. He, Y. Zhang, Z. Guo and L. Zhu, *Chem. Lett.*, 2000, 1030.
35 A. Caubet, V. Moreno, E. Molins and C. Miravitlles, *J. Inorg. Biochem.*, 1992, **48**, 135.